STATISTICALLY ASSISTED FLUID IMAGE REGISTRATION ALGORITHM - SAFIRA

Caroline C. Brun*[1], Natasha Lepore*[1,2], Xavier Pennec[3],
Yi-Yu Chou[1], Agatha D. Lee[1], Marina Barysheva[1], Greig I. de Zubicaray[4],
Katie L. McMahon[4], Margaret J. Wright[5], Paul M. Thompson[1]

[* equal contribution]

[1] Laboratory of Neuro Imaging, Department of Neurology, UCLA, Los Angeles, CA 90095, USA

[2] Children's hospital, University of South California, Los Angeles, CA, 90027, USA

[3] Asclepios Research Project, INRIA, 06902 Sophia-Antipolis Cedex, France

[4] Centre for Magnetic Resonance, University of Queensland, Brisbane, Queensland, 4072, Australia

[5] Genetic Epidemiology Lab, Queensland Institute of Medical Research, Queensland 4029, Australia

ABSTRACT

In this paper, we develop and validate a new Statistically Assisted Fluid Registration Algorithm (SAFIRA) for brain images. A non-statistical version of this algorithm was first implemented in [2] and re-formulated using Lagrangian mechanics in [3]. Here we extend this algorithm to $3D$: given $3D$ brain images from a population, vector fields and their corresponding deformation matrices are computed in a first round of registrations using the non-statistical implementation. Covariance matrices for both the deformation matrices and the vector fields are then obtained and incorporated (separately or jointly) in the regularizing (i.e., the non-conservative Lagrangian) terms, creating four versions of the algorithm. We evaluated the accuracy of each algorithm variant using the manually labeled $LPBA40$ dataset, which provides us with ground truth anatomical segmentations. We also compared the power of the different algorithms using tensor-based morphometry -a technique to analyze local volumetric differences in brain structure- applied to 46 3D brain scans from healthy monozygotic twins.

Index Terms— fluid, empirically-guided registration, Lagrangian mechanics

1. INTRODUCTION

Nonlinear registration is an image analysis procedure that matches one image or volume with another using biological or geometrical features present in both images.

Most registration algorithms select a similarity term (or cost function) - typically a distance between common anatomical or stereotaxic landmarks or an intensity-based measure over the whole image such as the squared-intensity difference. A regularizer compensates for the effects of this data fidelity term and enforces desirable properties in the deformation, such as smoothness, invertibility and inverse-consistency [9]. One method to account for these properties is to add the gradient of the similarity criterion as a distributed force force field in the mechanical equations that govern elastic [1] or viscous

fluid motions [4]. Other non-physical regularization models such as Gaussian filtering have been implemented, as these tend to be more efficient than the filters that are needed to implement continuum-mechanical operators [18].

As brain structure varies widely across subjects, and across the human lifespan, some registration methods have been developed to encode information on its natural variability [7, 6]. However, very few widely used volume registration methods incorporate empirical information on population variability in brain structure. The use of empirical statistics has been advocated many times, but none of the 14 nonlinear registration methods evaluated in [10] uses empirical information on brain variation during the registration process.

In fact, in the registration methods mentioned so far, a field of $3D$ displacement vectors is usually computed based on univariate data (one value per voxel) or from pre-defined landmarks. Consequently, as the information that can be consistently identified is limited, a realistic model is needed to interpolate the deformation to the rest of the brain. If such empirical information on brain variation was added in the registration process, the statistics of the modeled differences in brain structure would better match those that truly occur, possibly improving registration accuracy, stability, and convergence [8]. In some prior approaches, the statistics of the strain tensors were nonlinearly rescaled so that they could be used in a Demons-like registration algorithm [5]. Early studies by Gee and colleagues performed principal component analysis of intra-subject registration fields to develop an empirical model of brain shape, for use as a Bayesian prior to constrain registrations [8].

In this paper, we focused on fluid registration as it overcomes several known limitations of some continuum-mechanical elastic models, which are derived under small deformation assumptions and the resulting mappings may not be invertible if large image transformations are needed [4]. Fluid transformations remain diffeomorphic even for large deformations. We introduce a new Lagrangian approach, which incorporates different types (vector and tensor) of statistics on the expected deformations in the registration. This pro-

vides a mechanically meaningful framework to incorporate biological information in the registration process.

One application that we use to test our algorithm - for which it was primarily designed - is Tensor-Based Morphometry (TBM). TBM is an image analysis method that has been used successfully to detect morphometric differences associated with diseases [12] or normal brain development [16]. It consists of a registration step and a statistical analysis step. Our registration algorithm is well-suited for TBM as it regularizes the deformation tensors $\Sigma = J^T J = (Id+\nabla q)^T (Id+\nabla q)$ that are statistically analyzed in the second step of the method [11]. As such, there is a consistency between the subsequent statistical analysis of tensors arising from the registration, and the empirical information used to estimate the tensors in the first place.

Here, we first compare the accuracy of the different versions of the algorithm using the manually-labeled $LPBA40$ dataset. We also perform a Tensor-Based Morphometry analysis of brain MRI data from 23 monozygotic (MZ; identical) twin pairs to evaluate their statistical power in a research study. For each dataset, a first round of registrations was used to register the images using the non-statistical fluid code to obtain an initial distribution for the displacements and the deformation matrices. The mean and covariance matrices were computed, and a second round of registration incorporated either the vector-based, tensor-based or both statistics. In the TBM analysis, resemblances within pairs of twins were assessed by computing the intraclass correlation (ICC) of the determinant of the Jacobian matrices derived from the deformation fields. Both the accuracy and effects sizes were better for the vector-based statistical registration method.

2. REGISTRATION ALGORITHMS

2.1. Background

The $3D$ brain image volume is regarded as embedded in a deformable continuum-mechanical system; each voxel is seen as a particle of this deforming system. Its dynamic behavior may be modeled using Newtonian mechanics, as in [4]. In this case, the displacement of each particle (i.e., the voxels) is constrained by the Navier-Stokes equation for viscous fluid systems. Here, this equation is modified to integrate statistical data computed from the dataset. The Newtonian formulation does not clarify the mechanical role of the similarity and regularizing terms; on the other hand, the generalized framework determined by the non-conservative Lagrangian structure is flexible enough to contain two types of statistical information obtained from the dataset while remaining mechanically meaningful.

2.2. General formulation

The Lagrangian L can express the dynamic behavior of a system that is subject to conservative forces $L = T - V$. In the conservative case, $T(\dot{q})$ and $V(q)$ represent the kinetic energy and the potential energy of the system, respectively. q is the displacement, and $\dot{q}$ is the velocity of the system. One way to find the Lagrangian L is to examine its integral, called the action, $\mathcal{S}$ ($\mathcal{S} = \int_{t_0}^{t_1} L dt$). The paths followed by a mechanical system between the times t_0 and t_1 are the ones that minimize the action.

When the system is subjected to non-conservative forces, $\mathcal{S}$ changes to: $\mathcal{S} = \int_{t_0}^{t_1} L + W \, dt$ with $\delta W = \vec{F}.\delta\vec{r}$. δW is the work done by the non-conservative force $\vec{F}$ during the virtual displacement $\delta\vec{r}$, i.e., a variation associated with the possible body position $\vec{r}$, and not the actual solution $\vec{r}(t)$ ($\vec{r}$ is chosen so that the force $\vec{F}$ remains constant during the displacement $\delta\vec{r}$ and depends only on q). To find the path followed by the dynamic system (minimization of the action), $\delta\mathcal{S}$ can be derived as

$$\delta\mathcal{S} = \int_{t_0}^{t_1} \delta L + \delta W \, dt = 0$$

Hence, $\left(\dfrac{\partial L}{\partial q}\right) - \dfrac{d}{dt}\left(\dfrac{\partial L}{\partial \dot{q}}\right) + \vec{F}\left(\dfrac{\partial \vec{r}}{\partial q}\right) = 0;$ \hfill (1)

(see [17] for more details). This dynamic equation defines the movement of a non-conservative system at each time t.

2.3. Definition of the non-statistical version of algorithm

Here and in our previous work [2], the similarity between a template and the deforming image is defined by the sum of squared intensity differences (SSD) criterion: $Cost = Sim(I, J \circ q) = \int (I(x) - J(q(x))^2 dx$, but any other image similarity criterion could be used. In [2], we combined the fluid and Riemannian frameworks to create a so-called isotropic Riemannian fluid registration algorithm. At each voxel, for each time step Δt, the regularizer and image similarity cost terms were optimized to find the velocity $\dot{q}$ according to the equation (1) with:

1- $\dfrac{d}{dt}\left(\dfrac{\partial L}{\partial \dot{q}_j}\right) = \dfrac{d\dot{q}(q,t)}{dt} = \dfrac{d}{dt}\left(\dfrac{\partial}{\partial \dot{q}}\left(\dfrac{1}{2}||\dot{q}||_2^2\right)\right)$

2- $\dfrac{\partial L}{\partial q} = \nabla_q Cost(I, J, q)$ 3- $\vec{F}\left(\dfrac{\partial \vec{r}}{\partial q}\right) = \alpha\nabla_{\dot{q}} Reg_{riem}(\dot{q}) + \beta\dot{q}$

Hence, we have the following expressions:

1- Kinetic energy: $T = \frac{1}{2}||\dot{q}_j||_2^2$
2- Potential Energy: $V = Cost(q)$
3- Nonconservative energy: $V_{\vec{F}1} + V_{\vec{F}2} = \frac{1}{2}\beta||\dot{q}||_2^2 + \alpha Reg_{Riem}(\dot{q})$

Reg_{Riem} constrains the deformation of one image into another by acting on the rate of strain $\Sigma_{\dot{q}}$ rather than on the deformation matrix Σ (as was the case in [13]). Riemannian metrics are more appropriate than Euclidean ones, as the deformation tensors Σ's do not form a vector space but a cone in the vector space of 3x3 matrices, and standard Euclidean operations cannot be applied.

2.4. Statistical formulation

Given a dataset, we execute a first round of registrations to compute the statistics needed for the statistical regularization, i.e., that will be incorporated in the regularizing (non-conservative) terms. For each image from our dataset, we apply the non-statistical algorithm (see previous paragraph) to obtain a distribution of vector fields, from which we compute the covariance of the deformation tensors, Σ, and the covariance of the displacement fields, $\vec{q}$. $V_{\vec{F}1}$ and $V_{\vec{F}2}$ can be changed into their statistical versions using Mahalanobis distances.

The first non-conservative regularizing term can be modified as:

$$V_{\vec{F}2} = \frac{1}{4} \int Vect(W_{\dot{q}} - \bar{W}_{\dot{q}}) Cov^{-1} Vect(W_{\dot{q}} - \bar{W}_{\dot{q}})^T$$

Here $W_{\dot{q}} = log(\Sigma_{\dot{q}})$, and to avoid any bias, we choose to keep the average rate of strain $\bar{W}_{\dot{q}} = \frac{1}{N} \sum_i log(\Sigma_{\dot{q}_i})$ equal to zero at all times. The covariance Cov is computed using deformation tensors Σ_q. Using $\Sigma_{\dot{q}}$ would be equivalent because q and $\dot{q}$ are collinear to each other.

The other non-conservative term can also be modified to include the covariance of the displacements. The Euclidean norm $||.||_2$ is replaced by a Mahalanobis distance in $V_{\vec{F}1}$:

$$V_{\vec{F}1} = ||\dot{q}_j||^2 = \dot{q}_j^T cov_{q_j}^{-1} \dot{q}_j$$

with $cov_{q_j} = \frac{1}{N} \sum_i (q_i - \bar{q}_j)^T (q_i - \bar{q}_j)$, the covariance of the displacements q at a voxel j across the images i. This non-conservative term may be interpreted as a Rayleigh dissipation term. In fact, it is proportional to the quadratic velocity.

The algorithm can include both of the previous types of statistical data (vector- + tensor-based statistical version), the information on the Σ's only (tensor-based version), information on the displacement fields q only (vector-based version) or neither of them (non-statistical version of the algorithm).

3. DATA AND ANALYSIS

3.1. Data and preprocessing

3D $T1$-weighted images were acquired from 23 pairs of monozygotic (MZ) (11 male and 12 female pairs) using a $4T$ Bruker Medspec whole body scanner (rapid gradient echo (*MP-RAGE*) sequence) at the Center for Magnetic Resonance (University of Queensland, Australia). Another scan was identically performed on a subject who was not part of the genetic study, but whose scan was used as a template (target brain) for the registration. The age range for the subjects was $22 - 25$ years. All scans were then aligned to the ICBM53 template using 9-parameter registration (i.e., translational and rotational alignment, allowing scaling in 3 independent directions - *FMRIB*'s Linear Image Registration Toolbox. The $LPBA40$ brain MRI dataset was used to validate registration accuracy. Details can be found at `http://www.loni.ucla.edu/~shattuck/resources/lpba40/`.

3.2. Accuracy of volume quantification

As our algorithm was primarily developed to study volume and shape differences between subjects and groups in morphological studies such as TBM, we first estimated how the incorporation of different types of statistics influenced the results of volume estimation. We randomly chose a subject from the $LPBA40$ dataset as a template and registered all the other MRI scans to this template using the 3 independent versions of our algorithm (non-statistical, tensor- and vector-based). Then, we applied the vector field, obtained from each subject's registration to the template, to the corresponding labeled image (for each of the subjects, 56 structures, or regions of interest ROIs, were delineated manually). Each registered labeled image was compared to the manually segmented labeled template (ground truth segmentation). Volume differences between the template T_r and each subject S_r were reported for each region and averaged across the population. The volume similarity coefficient V_s was defined as [10]: $V_s = 2\frac{\sum (|S_r| - |T_r|)}{\sum (|S_r| + |T_r|)}$. For this measure, smaller values denote a lower segmentation error, and a more accurate quantification of substructure volumes.

3.3. Scalar values and heritability measures

The statistical power of the four algorithm variants was compared using a morphometry study. To measure the anatomical resemblance between MZ twin pairs, we computed the voxelwise intraclass correlation coefficient (ICC) in the cerebrum, according to the equation: $ICC = \frac{\sigma_b^2}{(\sigma_b^2 + \sigma_w^2)}$. σ_b^2 is the pooled variance between pairs and σ_w^2 is the variance within pairs. These ICC measures were computed from the Jacobian determinant at each voxel in the registered maps, which is an index of the regional volume of specific structures, relative to the standard template. As such, the ICC represents how similar brain structure volumes are between twins. Higher values mean that volumes are more correlated across members of a twin pair. We did not want to assume that the data, $det(J)$, was normally distributed across subjects, so we computed p-values at each voxel with a voxelwise permutation test, to establish a null distribution for the ICC statistics at each voxel [14].

4. RESULTS

4.1. Estimating the volume conservation

Figure 1 shows the volume quantification error, V_s, for all ROIs. Blue colors indicate small volume difference between the registered label and the manually defined ground truth label, whereas red colors indicate large differences between the volume of the deformed segmentation and the manually defined ground truth. Results are shown for the three independent versions of the algorithm (non-statistical, vector-based and tensor-based statistics). Overall, incorporating vector-based statistics on the deformation field during the registra-

tion improves volumetric matching, and makes volume quantification more accurate. This is the especially clear for subcortical gray matter structures, such as the caudate and putamen.

4.2. Significance of the Intraclass Correlation

The significance of the ICC is displayed as 3D maps for the whole cerebrum in **Figure 2** - top panel. The anatomical pattern is consistent across all methods. Subcortical structures, white matter and ventricles are influenced by genetic differences across individuals. Similar patterns of resemblance are found with all four versions, but the signal is more powerful when the vector-based algorithm is used for the registration step. To better quantify the difference in power, cumulative distribution functions were plotted (**Figure 2** - bottom panel), based on the $p$values for the ICC and are consistent with the previous results.

5. CONCLUSION

Here we combine the advantages of a large-deformation fluid matching approach with empirical statistics on population variability in anatomy. Our registration algorithm, called SAFIRA, was mathematically formulated using a *non-conservative Lagrangian* approach. Overall, the vector-based statistical method (0th-order statistics) showed the greatest improvement in detection sensitivity and accuracy versus the non-statistical Riemannian fluid or the tensor-based (1st-order statistics) code.

6. REFERENCES

[1] Bajcsy et al., *Comp Vis Graph Image Process*, 46(1), (1989) 1–21

[2] Brun et al., *MICCAI*, New-York, USA, (2008) 914–921.

[3] Brun et al., *ISBI*, Boston, MA, USA, (2009) 975–978

[4] Christensen et al. *IEEE TIP*, 5(10), (1996) 1435–1447

[5] Commowick, *MICCAI*, CA, USA, 8(2), (2005) 927–934

[6] Durrleman et al., *MedIA*, 13(5), (2009) 793–808

[7] Fillard et al.,*NeuroImage*, 34(2), (2007) 639–650

[8] Gee, J.C., *Pattern Recognit*, 1999

[9] Holden, M., *IEEE TMI*, 27(1), (2008), 111–127

[10] Klein et al., *NeuroImage*, 46(3), (2009) 786–802

[11] Leporé et al., *IEEE TMI*, 27(1), (2008) 129–14

[12] Leporé et al., *NeuroImage*, (2009) July

[13] Pennec et al., *MICCAI*, CA, USA, 8(2), (2005) 943–950

[14] Nichols et al., *Hum Brain Map*, 15(1), (2002) 1–25

[15] Shattuck et al., *MedIA*, 6(2), (2002) 129–141

[16] Thompson et al., *Nature*, 404(6774), (2000) 190–193

[17] Tveter, F.T., *Celestial Mechanics and dynamical astronomy*, 60(4), (1994) 409–419

[18] Vercauteren et al., *MICCAI*, New York, USA, 1, (2008), 754–761
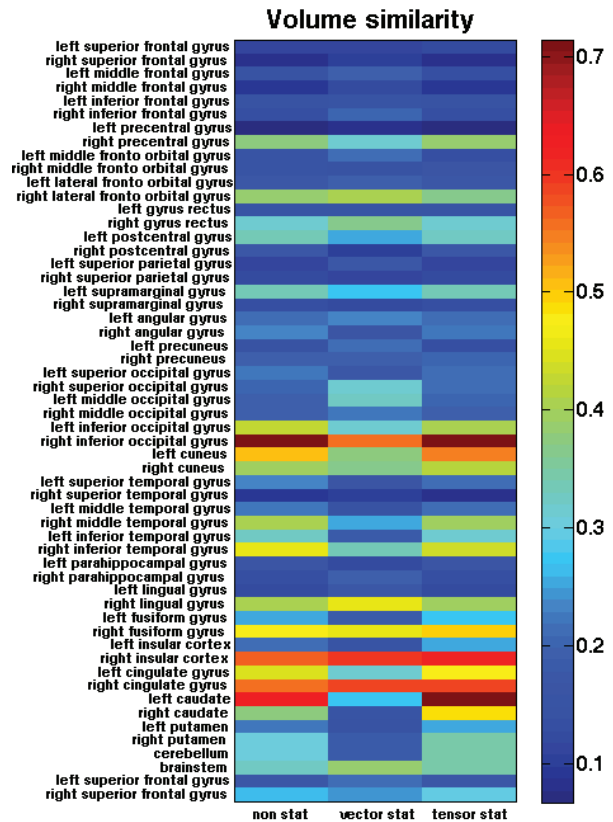
Fig. 1. Volume Quantification Error. Blue colors show better registration for the algorithm using vector-based statistics (middle column).
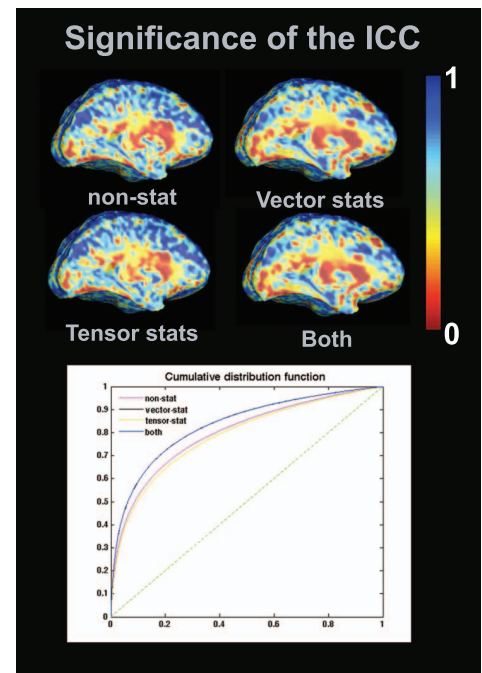
Fig. 2. **Top**: Significance of the ICC (log scale - $p = 0.05$ corresponds to yellow). **Bottom**: Corresponding cumulative distribution functions.